

## Comparison of Nitrogen Core and Ethylenediamine Core Starburst Dendrimers through Photochemical and Spectroscopic Probes

Steffen Jockusch,<sup>†</sup> Jenny Ramirez,<sup>†</sup> Kunal Sanghvi,<sup>†,§</sup> Robert Nociti,<sup>†,||</sup> Nicholas J. Turro,<sup>\*,†</sup> and Donald A. Tomalia<sup>‡</sup>

Department of Chemistry, Columbia University, New York, New York 10027, and Michigan Molecular Institute, Midland, Michigan 48640

Received January 12, 1999; Revised Manuscript Received April 26, 1999

**ABSTRACT:** The surface properties of ammonia core and ethylenediamine core poly(amidoamine) starburst dendrimers (N-SBD and EDA-SBD, respectively) were comparatively investigated, by employing photochemical and spectroscopic probes. Photoinduced electron-transfer quenching of tris-(2,2'-bipyridyl)ruthenium(II) chloride by methyl viologen on the SBD, monitored by fluorescence spectroscopy, was utilized to probe the negatively charged dendrimer surface. Electron-transfer quenching was found to be enhanced when the donor and acceptor are adsorbed on later generation dendrimers. Adsorption and aggregation of organic dyes, such as methylene blue and fluorescein, on negatively and positively charged dendrimers, respectively, were studied by applying UV-vis and fluorescence spectroscopy. The aggregation of the dyes depended strongly on the SBD generation. For the later generation SBDs, aggregation was found to occur more readily. Both photochemical and probe techniques allowed nearly identical conclusions for the external surface of the two different core dendrimers (N-SBD and EDA-SBD); i.e., the surface properties of both dendrimer types change qualitatively at approximately generation 3 from an "open" to a "closed" structure, as predicted by computational investigations of the full generations. These results suggest that earlier findings from applications involving N-SBD can be applied to more readily available EDA-SBD.

### Introduction

Starburst dendrimers are a novel class of macromolecules possessing a well-defined molecular composition and constitution. The molecular architecture of a starburst dendrimer is created by stepwise attachment of repeat unit layers or branches, termed generations, on a central core such as ammonia (N-SBD) or ethylenediamine (EDA-SBD).<sup>1–3</sup> The branches and external surface groups used in this work are shown in Scheme 1. When a dendrimer terminates with an amine function, it is termed a full ( $G = n.0$ ) generation; when a dendrimer molecule terminates with a carboxylate function, it is termed a half ( $G = n.5$ ) generation.

In nearly all previous studies using N-SBDs, photochemical and spectroscopic probe methods showed that the adsorption behavior of small molecules on the external surface allowed a consistent classification of the N-SBD into two groups: "earlier" generations (e.g., 2.5-N-SBD or less) possessing different adsorption properties than the "later" generations (e.g., 3.5-N-SBD and greater).<sup>4</sup> A model to explain the differences between the earlier and later generations was formulated and based on the notion that the earlier generations possess an open "starfish" surface structure, whereas the later generations possess a more closed and nearly spherical external surface structure. This model has been confirmed repeatedly for N-SBDs by various techniques, including fluorescence and optical absorption probes (pyrene,<sup>5</sup> metal complexes,<sup>6,7</sup> adsorption and aggregation of organic dyes<sup>8,9</sup>) and EPR techniques<sup>10,11</sup> as well as molecular simulations.<sup>1</sup>

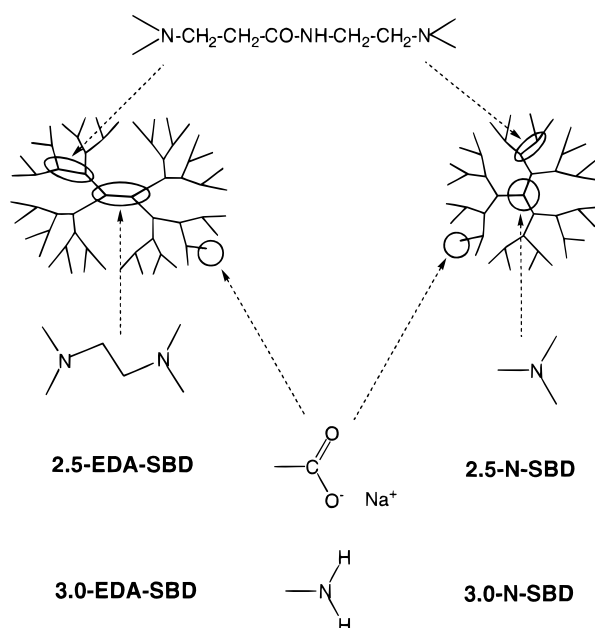
<sup>†</sup> Columbia University.

<sup>‡</sup> Michigan Molecular Institute.

<sup>§</sup> Present address: Bronx High School of Science, New York, NY.

<sup>||</sup> Present address: George Washington High School, New York, NY.

### Scheme 1. Structure of Starburst Dendrimers



An important basic science issue arises as to the nature of the external dendrimer surface as a function of the central core to which the branches are grafted. This issue is also a practical one, since the availability of a range of N-SBDs has been limited to research samples available to a very restricted number of research groups. Recently, however, EDA-SBDs (Scheme 1) have become commercially available for use by the research community in general. The issue now arises as to the impact of the central core on the external surface properties of dendrimers and the extent to which the extensive measurements and conclusions based on N-SBD may be transferred to EDA-SBD. To compare

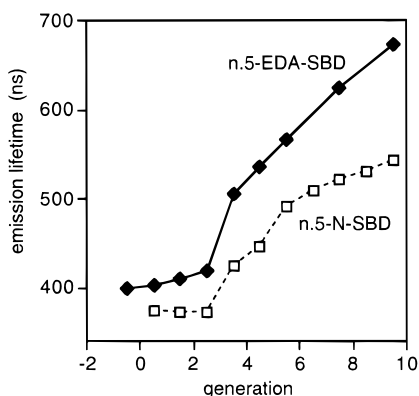


**Figure 1.** Emission lifetimes of  $\text{Ru}(\text{bpy})_3^{2+}$  ( $20 \mu\text{M}$ ) monitored at 610 nm and 23 °C in air-saturated aqueous solutions in the presence of different generations of *n.5*-EDA-SBD or *n.5*-N-SBD ( $20 \mu\text{M}$ ). The curve for *n.5*-N-SBD represents data from ref 7.

earlier findings from applications involving N-SBD with the results of the EDA-SBD, a systematic comparison of the surface properties between N-SBD and EDA-SBD is necessary. Therefore, in this study we applied a number of probe techniques, successfully used for N-SBD, to EDA-SBD.

### Experimental Section

The synthesis and characterization of N-SBDs and EDA-SBDs have been previously described in detail.<sup>1,2</sup> Methylene blue (MB) (Aldrich) was recrystallized from ethanol-water (4:1, v/v). Tris(2,2'-bipyridyl)ruthenium(II) chloride ( $\text{Ru}(\text{bpy})_3\text{Cl}_2$ ) (Aldrich), methyl viologen dichloride ( $\text{MVCl}_2$ ) (Aldrich), and fluorescein (FL) (Aldrich) were used as received.

The UV-vis spectra were measured on a HP 8452A diode array spectrophotometer using quartz cells with path lengths of 1.0 cm. Emission spectra were recorded either on a Spex Fluorolog 1680 0.22m double spectrometer or a Spex FluoroMax-2 spectrometer using quartz cells with path lengths of 1.0 cm. All measurements were performed at 23 °C with air saturated solutions in Millipore-filtered water.

The emission lifetime of  $\text{Ru}(\text{bpy})_3^{2+}$  in the presence of dendrimers was measured with a laser flash photolysis system employing pulses (532 nm, ca. 8 ns) from a Continuum Surelite I Nd:YAG laser and a computer-controlled detection system described elsewhere.<sup>12</sup>

### Results and Discussion

#### Photoluminescence and Electron-Transfer Quenching of $\text{Ru}(\text{bpy})_3^{2+}$ with $\text{MV}^{2+}$ on *n.5*-SBD.

The first probe method employed involves the response of photoluminescence to binding to the external surface of N-SBD or EDA-SBD. Positively charged probe molecules such as  $\text{Ru}(\text{bpy})_3^{2+}$  can be adsorbed at the negatively charged surface of *n.5*-SBD.<sup>7</sup> Photoexcited  $\text{Ru}(\text{bpy})_3^{2+}$  luminesces from the metal-to-ligand charge-transfer (MLCT) excited state upon excitation at 610 nm. Laser excitation (532 nm) was employed to photoexcite  $\text{Ru}(\text{bpy})_3^{2+}$  in air saturated aqueous solutions in the absence and in the presence of different generations of *n.5*-EDA-SBD. Emission lifetimes were measured by laser flash photolysis methods, and the results are shown in Figure 1.

The measured lifetimes of excited  $\text{Ru}(\text{bpy})_3^{2+}$  in the presence of early generations (0.5–2.5) are very close to those reported for  $\text{Ru}(\text{bpy})_3^{2+}$  in the absence of SBD ( $\tau_0 = 410$  ns). However, for higher generations ( $\geq 3.5$ -EDA-SBD), the emission lifetimes increase steadily (to values approaching 700 ns) with increasing

dendrimer generation. An equivalent effect was observed for *n.5*-N-SBD and is shown for comparison in Figure 1.<sup>7</sup> The increasing lifetime is explained in terms of strong adsorption of the complex to the external dendrimer surface starting at generation 3.5. The adsorbed probe may have a longer lifetime because of several factors such as decreased susceptibility against oxygen quenching<sup>6</sup> to the electrostatically bound  $\text{Ru}(\text{bpy})_3^{2+}$  with increasing dendrimer generation. This oxygen quenching was studied in detail for tris(1,10-phenanthroline)ruthenium(II) chloride in the presence of different generation dendrimers.<sup>6</sup> The previously reported data for *n.5*-N-SBD<sup>7</sup> are shown in Figure 1 for comparison and the trends are seen to be in good qualitative agreement with the results for the EDA-SBD. Since the small differences between both series of dendrimers (N-SBD and EDA-SBD) could be caused by the different experimental techniques and fitting routines, the differences are therefore not considered to be significant, and the two systems are considered to have essentially quantitatively equivalent responses to the probe method employed.

The second probe method employed involves the quenching of the luminescence of  $\text{Ru}(\text{bpy})_3^{2+}$  by  $\text{MV}^{2+}$ , which has been well established to occur via an electron-transfer mechanism.<sup>13–15</sup> In homogeneous aqueous solutions, a bimolecular rate constant of  $4.0 \times 10^8 \text{ M}^{-1} \text{ s}^{-1}$  was observed, which is in good agreement with previously published values.<sup>7,16</sup> Since  $\text{MV}^{2+}$  is positively charged, it possesses, as does the metal complex, a strong electrostatic affinity to the surface of the negatively charged *n.5*-SBD. When both  $\text{Ru}(\text{bpy})_3^{2+}$  and  $\text{MV}^{2+}$  are adsorbed on the same dendrimer molecule, photoinduced electron-transfer quenching is expected to be enhanced compared to that in the homogeneous solution, because the dendrimer acts as a host which organizes the system and allows  $\text{Ru}(\text{bpy})_3^{2+}$  and  $\text{MV}^{2+}$  to behave as a correlated reactive pair on a single surface.

Luminescence quenching experiments involving *n.5*-EDA-SBD were performed as previously described for *n.5*-N-SBD.<sup>7</sup> The decrease in the emission intensity of  $\text{Ru}(\text{bpy})_3^{2+}$  as a function of added  $\text{MV}^{2+}$  was monitored by steady-state fluorescence spectroscopy in the presence of different generations of *n.5*-EDA-SBD. Stern-Volmer treatment of the emission intensities showed a linear dependence until at least 50% quenching of the original emission intensity was achieved. However, curvature of the plot is observed above a certain amount of quencher. This could be caused by several factors, such as the displacement of  $\text{Ru}(\text{bpy})_3^{2+}$  by  $\text{MV}^{2+}$  on the dendrimer, which is expected to occur at high  $\text{MV}^{2+}$  concentrations. Figure 2 shows the slopes of the linear portion of the Stern-Volmer plots (Stern-Volmer constants,  $K_{\text{sv}}$ ) as a dependence on the generation of *n.5*-EDA-SBD, as well as the data points for *n.5*-N-SBD previously measured.<sup>7</sup> Agreement between the results is excellent and parallels that found for the lifetime probe (Figure 1).

For the low generations of dendrimer ( $G = 2.5$ ), the values of  $K_{\text{sv}}$  are very similar to those obtained in homogeneous solution. This can be explained by the small size and open structure of these early dendrimers, since both  $\text{Ru}(\text{bpy})_3^{2+}$  and  $\text{MV}^{2+}$  cannot fit on one dendrimer molecule (see schematic representation in Figure 2). For the later generations (3.5–7.5) Stern-Volmer constants several orders of magnitude higher

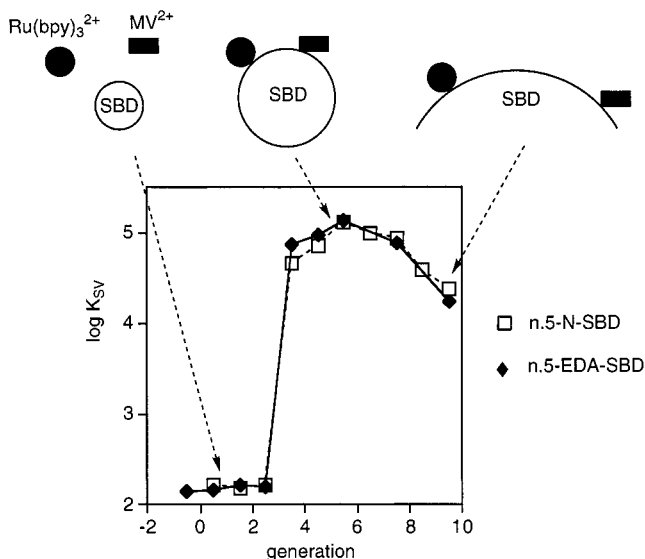


**Figure 2.** Stern–Volmer constants ( $K_{sv}$ , from steady-state emission intensity measurements) for the quenching of  $Ru(bpy)_3^{2+}$  ( $5 \mu M$ ) by  $MV^{2+}$  at  $23^\circ C$  in air-saturated aqueous solutions in the presence of different generations of  $n.5-EDA-SBD$  or  $n.5-N-SBD$  ( $5 \mu M$ ). The curve for  $n.5-N-SBD$  represents data from ref 7.

than those of earlier generations were observed, indicating a strong interaction between dendrimers,  $Ru(bpy)_3^{2+}$ , and  $MV^{2+}$ . The  $Ru(bpy)_3^{2+}$  luminescence was quenched effectively by  $MV^{2+}$  bound to the SBD surface because of the binding induced proximity of the excited molecule and a quencher (see schematic representation in Figure 2). Interestingly, in the case of the very large dendrimers (8.5 and 9.5) the Stern–Volmer constants decrease. This could be caused by the larger surface area of generation 9.5.  $Ru(bpy)_3^{2+}$  and  $MV^{2+}$  are probably more separated than in case of dendrimers of generation 5.5 (see schematic representation in Figure 2).

In conclusion, both a photoluminescence probe and a photochemical probe demonstrate that a change in dendrimer structural features occurs between generation 2.5 and 3.5 for both dendrimer types  $n.5-N-SBD$  and  $n.5-EDA-SBD$ . Importantly, any distinction between these two different dendrimers is essentially negligible as measured by the probe techniques.

#### Adsorption and Aggregation of MB on $n.5-SBD$ .

A third probe method involves the adsorption and aggregation of cation dyes on the external surface of EDA–SBD. When cationic organic dyes are adsorbed on negatively charged polyelectrolytes, aggregation of the dyes is sometimes observed. In addition to the electrostatic forces which bind the opposite charges of the polyanion and cation to each other, the self-organization of dye aggregates is promoted by at least two forces: dispersion forces due to the interaction between the  $\pi$ -systems of the dyes<sup>17</sup> and hydrophobic effects.<sup>18</sup> For aggregates to form and to be stable, the sum of these forces must be larger than the electrostatic repulsion between the positive charges on the dye molecules.

The aggregation of MB has been shown<sup>19</sup> to occur in the presence of polyanions to form large aggregates of MB bound to the surface of the polyanion. This aggregation can be readily detected by a hypsochromic shift of the absorption to the monomers and dimers and serves as a probe technique for the aggregation and adsorption of dyes on polyions and therefore as a probe of the

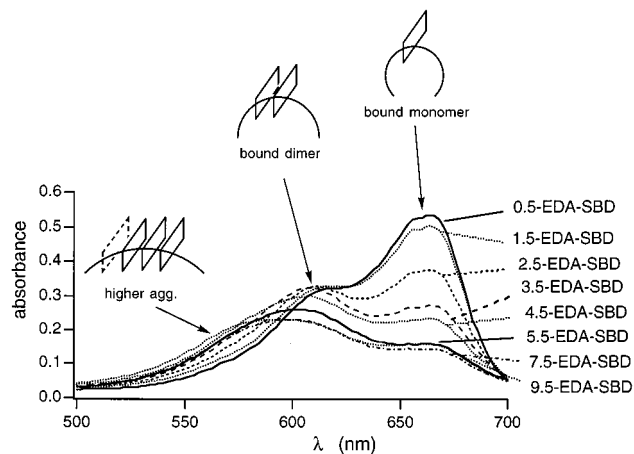


**Figure 3.** Optical absorption of MB ( $1 \times 10^{-5} M$ ) at the concentration of  $n.5-EDA-SBD$ s of the minimum absorbance at 666 nm (see Figure 4).

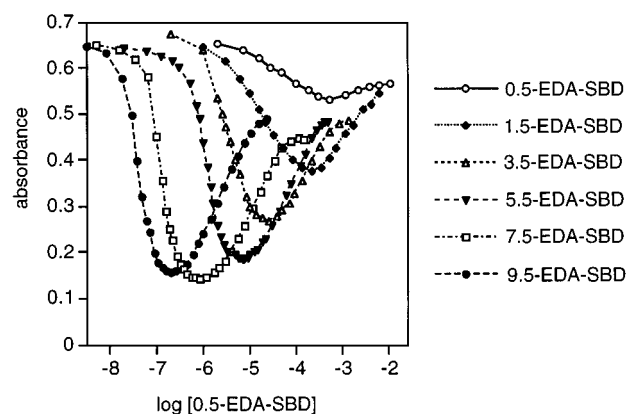


**Figure 4.** Optical absorption at 666 nm of the MB/ $n.5-EDA-SBD$  system for different generations of SBD.  $[MB] = 1 \times 10^{-5} M$ .

structure of polyions. We employed this probe technique to investigate the aggregation of MB on the external surface of  $n.5-N-SBD$ .<sup>8</sup> Previously, we have shown that the adsorption and aggregation of organic dyes such as MB can be used to probe surface properties of ammonia core  $n.5-SBD$  ( $n.5-N-SBD$ ).<sup>8</sup> Here, we compare the results of this method to dendrimers with an ethylenediamine core ( $n.5-EDA-SBD$ ).

At  $[MB] = 1 \times 10^{-5} M$ , MB does not show significant dimerization or aggregation in aqueous solution (dimerization constant:  $4710 M^{-1}$ );<sup>20</sup> however, dimers and aggregates of MB on the surface of SBD were detected by UV–vis spectroscopy in the presence of  $n.5-EDA-SBD$  (Figure 3). For the absorbance at 666 nm, where the absorption of MB monomer dominates, the most significant change was observed. Therefore, this wavelength was selected to monitor the dimer/aggregation behavior. Figure 4 shows the dependence of the dimerization/aggregation on the concentration of  $n.5-EDA-SBD$  molecules. In all cases, the monomer absorption of MB decreases with increasing concentration of  $n.5-EDA-SBD$ , and dimers/aggregates were observed at wavelengths lower than 600 nm, indicating that MB forms aggregates on SBDs. At higher concentrations of  $n.5-EDA-SBD$ , MB becomes distributed on the dendrimer molecules at the expense of the MB aggregates. This causes an increase in optical absorption at 666 nm corresponding to MB monomers bound to dendrimers (Figure 4).



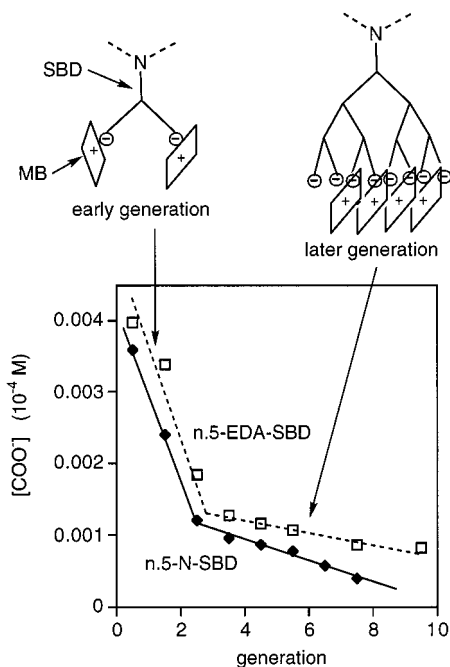


**Figure 5.** Concentration of SBD in surface groups at the minimum of the optical absorption at 666 nm (see Figure 4) vs the generation of *n*.5-EDA-SBD and *n*.5-N-SBD.

Figures 3 and 4 provide evidence that the MB aggregation depends strongly on the generation of dendrimers. For SBDs of later generation the aggregation occurs more readily and the number of MB molecules involved in one aggregate is larger than that observed for earlier generations (see schematic representation in Figure 3). The later conclusion is supported by examination of the minima of the plot of optical density vs dendrimer concentration (Figure 4). The minima are deeper for SBDs of later generations than for the earlier generations, indicating that the extent of aggregation is larger for later generation SBDs. The values of the minima in Figure 4 provide information about the concentration of SBDs when the largest aggregates of MB were formed. Figure 5 shows the dependence of this concentration on the generation of *n*.5-EDA-SBD. Note that a dramatic change occurs at generation 2.5.

Thus, the findings for MB aggregation on *n*.5-EDA-SBD are similar to those for *n*.5-N-SBD reported earlier.<sup>8</sup> Figure 5 also includes the aggregation dependence for *n*.5-N-SBD, which also shows an abrupt change at generation 2.5. We conclude that the aggregation of dyes as a probe tracks the same surface phenomenon as was tracked by the photoluminescence and photochemical probes (see schematic representation in Figure 5).

**Adsorption and Aggregation of Fluorescein on *n*.0-SBD.** Finally, a probe method to examine the external surface of the positively charged full generation SBDs was developed in order to investigate the external surface of full generation N-SBD with full generation EDA-SBD (See Scheme 1 for structures). Full generation SBDs (*n*.0-SBD), terminated with quaternary ammonia salts in aqueous solution, possess the characteristics of cationic polyelectrolytes. To probe their surface properties, the aggregation of negatively charged dyes was employed. Fluorescein (FL) was selected as a probe because it has been established that the transition dipole of FL dimers are not parallel-oriented. This causes a splitting of the dimer absorption into two

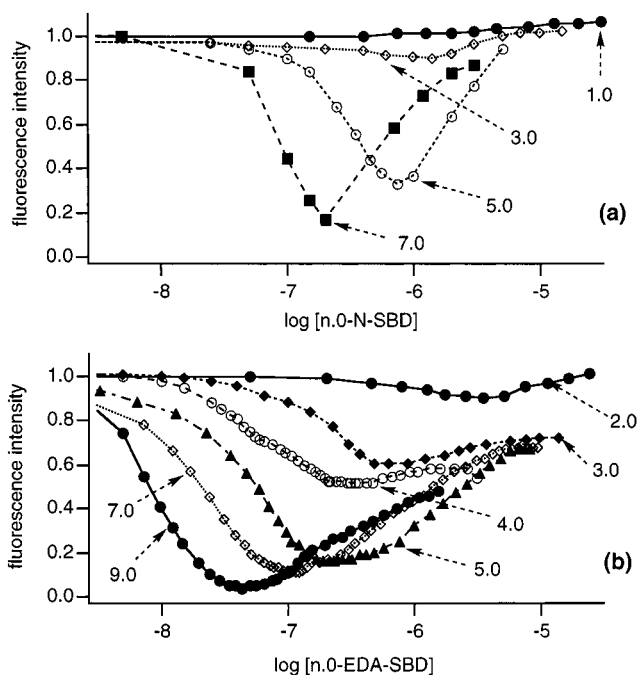


**Figure 6.** FL fluorescence intensity at the maximum vs the concentration of SBDs of different generations and different types of SBD. ([FL] =  $1 \times 10^{-5}$  M,  $\lambda_{ex}$  = 490 nm).

bands, one bathochromically shifted and one hypsochromically shifted relative to the monomer.<sup>21</sup>

The absorption spectra of higher aggregates are more complex. Consequently, to follow the aggregation of FL on *n*.0-SBD surfaces, optical absorption measurements cannot be used. But as was shown for the interaction of MB with *n*.5-N-SBD,<sup>8</sup> the adsorption and aggregation of some dyes can be followed by fluorescence spectroscopy if the dye fluorescence is self-quenched upon formation of dimers and aggregates.<sup>22</sup> As a monomer in aqueous solution, FL exhibits a fluorescence maximum at 515 nm. From steady-state measurements the fluorescence of the free FL in the bulk solution and the fluorescence of nonaggregated FL adsorbed on the surface of *n*.0-SBD can be detected. The steady-state fluorescence of the dimer and higher aggregates is negligible due to self-quenching.

Figure 6a depicts the results of the probe for aggregation of FL on *n*.0-SBD as a function of generation. With increasing concentration of *n*.0-SBD, aggregates of FL on the SBD surface were formed, leading to a decrease in the fluorescence intensity. Upon further increase in the concentration of SBD, FL becomes distributed on the SBD molecules at the expense of the FL aggregates. This causes an increase in the fluorescence intensity of monomers. The fluorescence maximum of bound dye monomers is shifted bathochromically depending on the dendrimer generation.

Parts a and b of Figure 6 show how the association and aggregation of FL with *n*.0-SBD strongly depended on the generation of the SBD. For both types, *n*.0-N-SBD and *n*.0-EDA-SBD, nearly no dye dimers or higher aggregates were formed for generation 0 to 2, due to the open structure of lower SBD generations. Figure 7 shows the minimum fluorescence that can be achieved upon addition of *n*.0-SBD of different generations. The remaining fluorescence is due to free dye monomer in solution or bound to SBD as monomer. Starting at generation 3, the fluorescence intensity has already decreased dramatically. This generation is the transi-

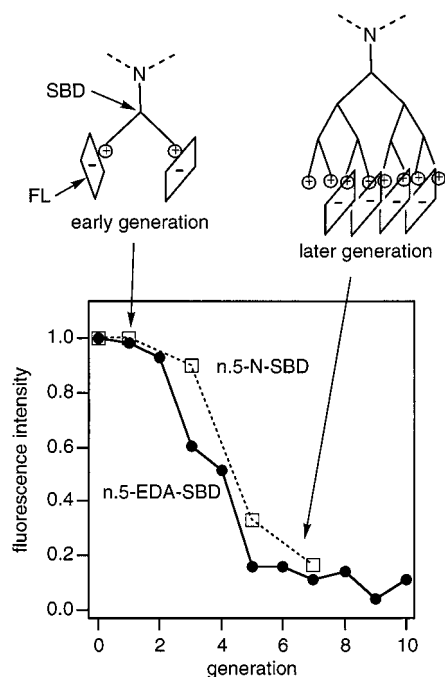


**Figure 7.** Fluorescence intensity at the minimum of the function shown in Figure 6 vs the generation of *n.5*-EDA-SBD and *n.5*-N-SBD.

tion point where the dendrimers show a closed surface structure. From Figure 7, again, the probe technique does not distinguish any significant difference between the adsorption behavior for the EDA-SBD or the N-SBD.

### Summary and Conclusion

The external surface properties of ammonia core and ethylenediamine core starburst dendrimers (N-SBD and EDA-SBD, respectively) were investigated. For the negatively charged *n.5*-SBD, probe techniques utilizing electron-transfer quenching of  $\text{Ru}(\text{bpy})_3^{2+}$  with  $\text{MV}^{2+}$  and aggregation of MB were used. Both techniques showed almost identical results for the two different dendrimer types investigated (*n.5*-N-SBD and *n.5*-EDA-SBD). Both dendrimer types change their surface properties at about generation 2.5 from an open to a closed structure.

For the positively charged full generation dendrimers (*n.0*-SBD), the aggregation of fluorescein on these dendrimers was used to investigate their surface properties. For both types of dendrimers (*n.0*-N-SBD and *n.0*-EDA-SBD), the structural change from an open to a closed structure occurs at approximately generation 3.

Therefore, we conclude that earlier findings from applications involving N-SBD can also be applied to EDA-SBD.

**Acknowledgment.** N.J.T. and S.J. thank the National Science Foundation (CHE93-13102) for its generous support of this research. D.A.T. thanks the

New Energy and Development Organization (NEDO) of the Ministry of International Trade and Industry of Japan (MITI) for its generous support and certain critical synthetic efforts. J.R. thanks NSF for a minority undergraduate fellowship. R.N. thanks the Research Corporation (HS) for support of the Secondary School Science Teachers program at Columbia.

### References and Notes

- (1) Tomalia, D. A.; Baker, H.; Dewald, J.; Hall, M.; Kallos, G.; Martin, S.; Roeck, J.; Ryder, J.; Smith, P. *Polym. J.* **1985**, *17*, 117.
- (2) (a) Tomalia, D. A.; Berry, V.; Hall, M.; Hedstrand, D. M. *Macromolecules* **1987**, *20*, 1164. (b) Tomalia, D. A.; Hall, M.; Hedstrand, D. M. *J. Am. Chem. Soc.* **1987**, *109*, 1601. (c) Padias, A. B.; Hall, H. K.; Tomalia, D. A.; McConnell, J. R. *J. Org. Chem.* **1987**, *52*, 5305. (d) Wilson, L. R.; Tomalia, D. A. *Polym. Prepr. (Am. Chem. Soc., Div. Polym. Chem.)* **1989**, *30*, 115. (e) Tomalia, D. A.; Naylor, A. M.; Goddard, W. A., III *Angew. Chem., Int. Ed. Engl.* **1990**, *29*, 138.
- (3) (a) Krohn, K. Starburst Dendrimers and Arborols. *Org. Synth. Highlights* **1991**, 378. (b) Amato, L. Trekking in the Molecular Forest. *Sci. News* **1990**, *138*, 298. (c) Newkome, G. R.; Moorefield, C. N.; Baker, G. R.; Johnson, A. L.; Behera, R. K. *Angew. Chem., Int. Ed. Engl.* **1991**, *30*, 1176. (d) Newkome, G. R.; Moorefield, C. N.; Baker, G. R.; Saunders, M. J.; Grossman, S. H. *Angew. Chem., Int. Ed. Engl.* **1991**, *30*, 1178. (e) Kim, Y. H.; Webster, O. W. *J. Am. Chem. Soc.* **1990**, *112*, 4592. (f) Hawker, C. J.; Wooley, K. L.; Fréchet, J. M. J. *J. Chem. Soc., Perkin Trans. 1* **1993**, 1287. (g) Newkome, G. R.; Young, J. K.; Baker, G. R.; Potter, R. L.; Audoly, L.; Cooper, D.; Weis, C. D. *Macromolecules* **1993**, *26*, 2394. (h) Newkome, G. R., Ed.; *Advances in Dendritic Macromolecules*; JAI Press: Greenwich CT, 1993.
- (4) The nomenclature of the N-SBDs was recently changed. The nomenclature used in this paper is the same as that previously used or  $n\text{-N-SBD} = 1 + n\text{-N-SBD}_{\text{old}}$ .
- (5) Caminati, G.; Turro, N. J.; Tomalia, D. A. *J. Am. Chem. Soc.* **1990**, *112*, 8515.
- (6) Turro, C.; Niu, S.; Bossmann, S. H.; Tomalia, D. A.; Turro, N. J. *J. Phys. Chem.* **1995**, *99*, 5512.
- (7) Moreno-Bondi, M. C.; Orellana, G.; Turro, N. J.; Tomalia, D. A. *Macromolecules* **1990**, *23*, 910.
- (8) Jockusch, S.; Turro, N. J.; Tomalia, D. A. *Macromolecules* **1995**, *28*, 7416.
- (9) Jockusch, S.; Turro, N. J.; Tomalia, D. A. *J. Inf. Rec.* **1996**, *22*, 427.
- (10) Ottaviani, M. F.; Bossmann, S.; Turro, N. J.; Tomalia, D. A. *J. Am. Chem. Soc.* **1994**, *116*, 661.
- (11) Ottaviani, M. F.; Turro, C.; Turro, N. J.; Bossmann, S. H.; Tomalia, D. A. *J. Phys. Chem.* **1996**, *100*, 13667.
- (12) McGarry, P. F.; Cheh, J.; Ruiz-Silva, B.; Hu, S.; Wang, J.; Nakanishi, K.; Turro, N. J. *J. Phys. Chem.* **1996**, *100*, 646.
- (13) Orellana, G.; Quiroga, M. L.; Braun, A. M. *Helv. Chim. Acta* **1987**, *70*, 2073.
- (14) Kalyanasundaram, K. *Coord. Chem. Rev.* **1982**, *46*, 159.
- (15) Hoffman, M. Z.; Bolletta, F.; Moggi, L.; Hug, G. L. *J. Phys. Chem. Ref. Data* **1989**, *18*, 219.
- (16) Chiorboli, C.; Indelli, M. I.; Scandola, M. A. R.; Scandola, F. *J. Phys. Chem.* **1988**, *92*, 156.
- (17) London, F. Z. *J. Phys. Chem.* **1930**, *B11*, 222.
- (18) Jordan, D. O.; Kurucsec, T.; Martin, M. L. *Trans. Faraday Soc.* **1969**, *65*, 612.
- (19) Shirai, M.; Nagatsuka, T.; Tanaka, M. *J. Polym. Sci., Polym. Chem. Ed.* **1977**, *15*, 2083.
- (20) Ruprecht, J.; Baumgaertel, H. *Ber. Bunsen-Ges. Phys. Chem.* **1984**, *88*, 145.
- (21) Arbeloa, L. *J. Chem. Soc., Faraday Trans. 2* **1981**, *77*, 1725.
- (22) Yuzhakov, V. I. *Russ. Chem. Rev. (Engl. Transl.)* **1979**, *48*, 1076.

MA990044W